Research Square

Preprints are preliminary reports that have not undergone peer review.
They should not be considered conclusive, used to inform clinical practice,
or referenced by the media as validated information.

Longitudinal plasma biomarkers and multimodal PET across APOE ε4 genotypes: a prospective cohort study

Mikko Koivumäki

mikkkoi@utu.fi

University of Turku

Anniina Snellman

University of Turku

Laura Ekblad

University of Turku

Andrea Benedet

University of Gothenburg

Henrik Zetterberg

University of Gothenburg

Juha Rinne

Turku University Hospital

Research Article

Keywords: Preclinical Alzheimer's disease, Apolipoprotein E ε4, Blood-based biomarkers, p-tau217, Glial fibrillary acidic protein, Neurofilament light chain, Synaptic biomarkers, Amyloid PET, Synaptic density, Neuroinflammation

Posted Date: November 1st, 2026

DOI: https://doi.org/10.21203/rs.3.rs-11294615/v1

License: This work is licensed under a Creative Commons Attribution 4.0 International License.
Read Full License

Additional Declarations: No competing interests reported.

Abstract

Background

In preclinical Alzheimer's disease (AD), longitudinal trajectories of blood-based biomarkers and their relationship to brain amyloid pathology, synaptic density and neuroinflammation in cognitively unimpaired individuals stratified by apolipoprotein E (*APOE*) ε4 genotype remain poorly characterized.

Methods

We measured plasma tau phosphorylated at threonine 217 (p-tau217), glial fibrillary acidic protein (GFAP), neurofilament light chain (NfL), synaptosomal-associated protein 25 (SNAP25) and neurogranin (NRGN) using the nucleic acid-linked immuno-sandwich assay (NULISA) platform at baseline (n = 60) and after 4.4 years (n = 45) in cognitively unimpaired older adults (*APOE* ε4/ε4, n = 19; ε4/ε3, n = 21; ε3/ε3, n = 20 at baseline). Longitudinal biomarker changes were analyzed using linear mixed-effects models. Associations with [^{11}C]PiB (amyloid) and [^{11}C]PK11195 (neuroinflammation) positron emission tomography (PET) at baseline and [^{11}C]UCB-J (synaptic density) PET were examined using multiple linear regression.

Results

GFAP increased over time in all genotype groups and NfL in the ε4/ε4 and ε3/ε3 groups, with no group differences in rate of change. Plasma p-tau217 was the only biomarker robustly associated with amyloid burden at both timepoints. Synaptic markers showed minimal longitudinal change and no association with synaptic density PET.

Conclusions

These findings support a model in which p-tau217 specifically tracks amyloid-driven pathological progression, while markers of neurodegeneration reflect broader age-related processes that are not associated with *APOE* genotype.

Background

Alzheimer's disease (AD) is characterized by a prolonged preclinical phase during which pathological changes accumulate in the brain years or decades before the onset of cognitive symptoms [1, 2]. Early detection of this phase has become a central goal of AD research, driven by the recognition that disease-modifying interventions are most likely to be effective before irreversible neuronal loss occurs [3]. The apolipoprotein E ε4 (*APOE* ε4) allele is the strongest common genetic risk factor for late-onset AD, with

homozygous carriers facing a substantially elevated lifetime risk and earlier age of onset compared to non-carriers [4, 5]. Characterizing how *APOE* genotype shapes the trajectory of AD-related pathology in cognitively unimpaired individuals is therefore critical for identifying those at greatest risk and for interpreting biomarker data in the context of clinical trials and prevention strategies.

Blood-based biomarkers have emerged as scalable and minimally invasive tools for tracking preclinical AD pathology [6]. Phosphorylated tau at threonine 217 (p-tau217) has attracted particular interest as a sensitive marker of amyloid-driven tau pathology, showing strong concordance with amyloid and tau PET in both clinical and preclinical populations [7]. Glial fibrillary acidic protein (GFAP) and neurofilament light chain (NfL) provide complementary information on astrogliosis and axonal injury respectively, and both have been associated with amyloid burden and disease progression [8–10]. More recently, synaptic biomarkers including synaptosomal-associated protein 25 (SNAP25) and neurogranin (NRGN) have been proposed as early indicators of synaptic dysfunction, a pathological feature closely linked to cognitive decline in AD [11–14]. However, whether these blood-based markers, assessed using high-sensitivity platforms, reflect the localized synaptic and neuroinflammatory changes detectable by positron emission tomography (PET) in cognitively unimpaired individuals remains unclear.

The ASIC-E4 study ("Beta-Amyloid, Synaptic loss, Inflammation and Cognition in healthy *APOE* ε4 carriers") was designed specifically to investigate the early interplay of these pathological features in cognitively unimpaired individuals stratified by *APOE* genotype [15]. Cross-sectional analyses from this cohort have previously demonstrated that fibrillar amyloid burden increases in an *APOE* ε4 gene dose-dependent fashion [16], that hippocampal synaptic density measured by [^{11}C]UCB-J PET is reduced in *APOE* ε4 homozygotes compared with non-carriers [17], and that blood biomarkers (BBM) of neurodegeneration show distinct associations with amyloid, medial temporal atrophy, and cerebrovascular pathology across genotype groups [18]. However, these cross-sectional findings do not address whether *APOE* genotype influences the rate of change in blood-based biomarkers over time, nor whether baseline imaging findings predict subsequent longitudinal biomarker trajectories.

To address this, we examined longitudinal changes in plasma p-tau217, GFAP, NfL, SNAP25, and NRGN over 4.4 years in a cohort of cognitively unimpaired older adults who are either *APOE* ε4 homozygotes, heterozygotes or non-carriers and assessed their relationship to baseline amyloid, neuroinflammation and synaptic density measured by [^{11}C]PiB, [^{11}C]PK11195, and [^{11}C]UCB-J PET, respectively.

Methods

Study design and participants

The study population consisted of cognitively unimpaired older adults (aged 60–75 years) recruited from the Turku region, Finland, via the Auria Biobank, as described in detail in previous study protocols and baseline reports [15–18]. The study was conducted in accordance with the Declaration of Helsinki and was approved by the Ethical Committee of the Hospital District of Southwest Finland. All participants

signed a written informed consent. The structure of the study is shown in Fig. 1. Initially, 60 participants were stratified based on their *APOE* genotype into three groups representing varying genetic risk for AD: *APOE* ε4 homozygotes (ε4/ε4), heterozygotes (ε4/ε3), and non-carriers (ε3/ε3). All participants underwent comprehensive neurocognitive testing to confirm their cognitively unimpaired status at enrollment. The baseline [¹¹C]PiB PET, [¹¹C]PK11195 PET, and blood sample cohorts included 60 individuals (19 ε4/ε4, 21 ε4/ε3 and 20 ε3/ε3). For synaptic density, [¹¹C]UCB-J PET was performed on a subset of 46 individuals (14 ε4/ε4, 16 ε4/ε3 and 16 ε3/ε3) on average 2.0 years later than [¹¹C]PiB PET and [¹¹C]PK11195 PET. Follow-up blood samples were collected from a further subset of 45 individuals (11 ε4/ε4, 16 ε4/ε3 and 18 ε3/ε3) for longitudinal analysis, with a mean follow-up time of 4.4 years (range: 3.5–5.1 years). The mean interval between the [¹¹C]UCB-J visit and the follow-up blood samples was 2.6 years (range 1.5–3.5 years). Baseline characteristics did not differ significantly between study completers and non-completers (Additional file 1: Table S1).

Blood biomarker measurements

Venous EDTA-plasma samples were acquired at baseline and follow-up after a 10–12 h fasting period. Samples were gently inverted 5–10 times, centrifuged (2200 × g, 10 min), aliquoted, and stored at − 80°C prior to biomarker analysis. The following biomarkers were quantified to assess different aspects of neurodegeneration and AD pathology, p-tau217 as a marker of tau pathology, GFAP as a marker of reactive astrogliosis, NfL as a measure of axonal damage, and NRGN, and SNAP25 as markers of synaptic integrity and dysfunction.

Plasma concentrations of p-tau217, GFAP, NfL, NRGN, and SNAP25, were quantified using the NULISA platform (Alamar Biosciences, Fremont, CA, USA). The NULISA assay is a high-sensitivity proteomic technology leveraging a proximity-based rolling circle amplification combined with next-generation sequencing readout. The platform utilizes a dual-antibody recognition mechanism, which reduces background noise and enables the detection of biomarkers at attomolar levels. All samples were analyzed in a single batch according to the manufacturer's instructions, with researchers blinded to the clinical and genetic data. Protein levels were quantified as NULISA Protein Quantification (NPQ), a $\log_2$-transformed relative abundance unit normalized to internal controls.

Brain imaging measurements

The PET imaging methods used in this study, including tracer synthesis, acquisition protocols, and image processing for [^{11}C]PiB, [^{11}C]PK11195, and [^{11}C]UCB-J, have been described in detail previously [15–17]. In short, to assess the underlying pathology of AD, participants underwent multi-tracer PET imaging at the Turku PET Centre using three distinct radioligands. [^{11}C]PiB was utilized to quantify beta-amyloid deposition, while [^{11}C]PK11195, which targets the 18-kDa translocator protein, was employed to evaluate neuroinflammation and glial activation. Additionally, [^{11}C]UCB-J was used to measure the density of the synaptic vesicle glycoprotein 2A as a proxy for synaptic integrity. All PET data were co-registered with

structural T1-weighted MRI scans to facilitate anatomical reference and region-of-interest (ROI) definition. Quantification of tracer binding was performed using specific reference tissue models: [^{11}C]PiB and [^{11}C]UCB-J uptake were expressed as Standardized Uptake Value Ratios (SUVRs) using the cerebellar cortex and centrum semiovale as reference regions, respectively, while [^{11}C]PK11195 binding was quantified as Distribution Volume Ratios (DVRs).

Brain image analysis

PET and MRI image preprocessing and analysis were performed using an automated pipeline at Turku PET Centre [19], which executed PET data frame by frame realignment, PET-MRI co-registration, FreeSurfer ROI parcellation, and PET data kinetic modeling. For all PET tracers, binding was quantified over a volume weighted cortical composite region of interest (ROI) including medial temporal cortex (including hippocampus, amygdala, and entorhinal cortex), prefrontal cortex, parietal cortex, lateral temporal cortex, precuneus, anterior cingulum, and posterior cingulum [17]. [^{11}C]PiB binding was quantified as SUVR for the 60 to 90 min post-injection period, using the cerebellar cortex as reference region. [^{11}C]PK11195 binding was quantified as DVR within 20–60 min post injection using a reference tissue input Logan's method, with the pseudo-reference region extracted using a supervised clustering algorithm [20, 21]. [^{11}C]UCB-J binding was quantified as SUVR for the 60- to 90-minute period post injection, using the centrum semiovale as reference region. Importantly, [^{11}C]PiB and [^{11}C]PK11195 PET scans were performed at the baseline visit, concurrent with baseline blood sampling, whereas [^{11}C]UCB-J PET was performed at a separate dedicated imaging visit (the UCB-J visit; see Fig. 1). Although all PET scans were originally planned to be acquired at the baseline visit, [^{11}C]UCB-J imaging was delayed due to tracer production difficulties and disruptions caused by the COVID-19 pandemic. The amyloid-, neuroinflammation-, and SV2A-PET results have been published in more detail elsewhere [16, 17].

Statistical analyses

Longitudinal changes in BBM were analyzed using linear mixed-effects models. The models included study group (ε4/ε4, ε4/ε3 and ε3/ε3), time (Baseline and Follow-up), and their interaction (Group*Time) as fixed effects to evaluate whether the rate of change differed between the groups. Age was included as a fixed covariate in all models, for GFAP also sex, and for NfL sex and BMI to account for their potential influence on biomarker levels. To account for the inherent correlation between repeated measurements within the same individual, subject ID was included as a random effect (random intercept). Post-hoc pairwise comparisons for significant effects were conducted using the Tukey-Kramer Honest Significant Difference (HSD). Model assumptions, including the normality of residuals and homoscedasticity, were verified through visual inspection of residual quantile (Q-Q) plots and residual-by-predicted plots. Statistical significance was set at $p < 0.05$.

To evaluate associations between baseline PET imaging measures and BBMs, both at baseline and follow-up, multiple linear regression was used. A separate model was fit for each BBM (GFAP, NfL, p-

tau217, SNAP25, NRGN), with PET measures as predictors and age, sex, BMI, and *APOE* ε4 count included as covariates to assess independent predictive value. Standardized Beta coefficients and point estimates with 95% confidence intervals were calculated to determine the strength and direction of the associations. Model fit was assessed using the adjusted R^2. Statistical significance was set at alpha = 0.05. All analyses were performed using JMP version 18 (SAS Institute Inc., Cary, NC) and visualizations using GraphPad Prism version 9.0.1 (GraphPad, San Diego, California, USA).

Use of large language models

An AI assistant (Claude, Anthropic) was used to check and edit the manuscript against the journal's formatting requirements; the authors reviewed all changes and take full responsibility for the content.

Results

Participants and baseline demographics

A total of 60 participants were included at baseline, categorized by *APOE* ε4 genotype into three groups: ε4/ε4 (n = 19), ε4/ε3 (n = 21), and ε3/ε3 (n = 20). As shown in Table 1, there were no significant differences between the groups regarding age (p = 0.75), sex (p = 0.91), education level (p = 0.37), or BMI (p = 0.86). The mean age across groups ranged from 67.3 to 68.3 years, and the cohort was predominantly female (60%–67%).

Table 1
Demographics of the participants

Group	**ε4/ε4**	**ε4/ε3**	**ε3/ε3**	**Group difference (p)**
Baseline				
n	19	21	20	
Age (years), mean (SD)	67.3 (4.74)	67.3 (4.90)	68.3 (4.55)	0.75
Sex (M/F), n (%)	7/12 (37/63)	7/14 (33/67)	8/12 (40/60)	0.91
Education, n (%)				0.37
Primary school	7 (37)	4 (19)	7 (35)	
Middle school	4 (21)	4 (19)	3 (15)	
High school	7 (37)	6 (29)	7 (35)	
College or university	1 (5)	7 (33)	3 (15)	
BMI (kg/m^2), mean (SD)	26.6 (4.48)	26.7 (3.46)	27.3 (4.96)	0.86
MMSE, median (IQR)	28 (27–29)	29 (28–30)*	29 (27–30)	**0.040**
[^{11}C]**PiB SUVR**	2.13 (1.61–2.83)	1.55 (1.43–2.02)	1.47 (1.38–1.66)*	**0.0024**
[^{11}C]**PK11195 DVR**	1.34 (0.77)	1.33 (0.52)	1.31 (0.58)	0.30
UCB-J visit				
n	14	16	16	
Sex (M/F), n (%)	6/8 (43/57)	4/12 (25/75)	6/10 (37/63)	0.64
BMI (kg/m^2)	26.2 (4.32)	26.3 (3.99)	27.9 (4.64)	0.49
MMSE	27.5 (27–29)	29 (28–30)	28.5 (27–30)	0.16
[^{11}C]**UCB-J SUVR**	4.20 (0.74)	4.39 (0.65)	4.63 (0.54)	0.24
Follow-up visit				
n	11	16	18	
Age (years), mean (SD)	70.0 (5.1)	70.7 (5.6)	73.0 (4.5)	0.78
Sex (M/F), n (%)	3/8 (27/73)	3/13 (19/81)	7/11 (39/61)	0.35

Group	ε4/ε4	ε4/ε3	ε3/ε3	Group difference (p)
Baseline				
Education, n (%)				0.52
Primary school	3 (27)	2 (13)	6 (33)	
Middle school	1 (9)	4 (25)	2 (11)	
High school	6 (55)	5 (31)	7 (39)	
College/University	1 (9)	5 (31)	3 (17)	
BMI (kg/m^2), mean (SD)	26.0 (4.3)	27.1 (3.8)	27.4 (4.7)	0.47
MMSE, median (IQR)	28 (26–29)	29 (29–30)	29(29–30)	0.066

Data are presented as mean (standard deviation) or median (interquartile range) depending on the distribution. Differences between groups were tested with one-way ANOVA with Tukey's honest significance test or Kruskal–Wallis test with Dunn's method for multiple comparisons for continuous variables. χ^2 test was used for testing categorical variables. P value presents overall difference between groups. Statistically significant pairwise differences compared to APOE ε4 homozygotes are indicated with an asterisk ($p < 0.05$) Abbreviations: BMI body mass index, DVR distribution volume ratio, MMSE mini-mental state examination, SUVR standardized uptake value ratio. n, number of unique participants. Bold p values indicate $p < 0.05$.

While baseline cognitive function measured by the MMSE showed a significant overall group difference ($p = 0.040$), median scores were high across all groups (28–29) and remained stable throughout the follow-up. Significant differences were observed in amyloid deposition as the [^{11}C]PiB SUVR was highest in the ε4/ε4 group (median 2.13) compared to the ε4/ε3 (median 1.55) and ε3/ε3 (median 1.47) groups ($p = 0.0024$). No significant differences were found in baseline [^{11}C]PK11195 DVR ($p = 0.30$) or in [^{11}C]UCB-J SUVR ($p = 0.24$). Participation remained relatively consistent through follow-up, though sample sizes decreased to n = 11, n = 16, and n = 18 for the ε4/ε4, ε4/ε3, and ε3/ε3 groups, respectively.

Longitudinal changes

Linear mixed model analysis showed that several biomarkers increased over the follow-up period, although the rate of change did not differ significantly between the study groups for any of the analyzed markers. Longitudinal increases were observed for plasma GFAP and NfL (Fig. 2 and Table 2). GFAP rose significantly in all three groups (ε4/ε4: $p = 0.0002$; ε4/ε3: $p < 0.0001$; ε3/ε3: $p < 0.0001$). No significant group-by-time interaction was found ($p = 0.96$), indicating that GFAP levels increased at a comparable rate across all groups. NfL concentrations increased significantly in ε4/ε4 ($p = 0.0204$) and ε3/ε3 ($p = 0.0235$), while ε4/ε3 showed a non-significant upward trend ($p = 0.0945$). There was no significant

difference between the groups (p = 0.72). For plasma p-tau217, a borderline significant increase was observed specifically in ε3/ε3 (LSMean difference = -0.176, p = 0.0505), whereas levels remained stable in ε4/ε4 and ε4/ε3 (Fig. 2 and Table 2). There was no significant difference between the groups (p = 0.24). No significant longitudinal changes or interaction effects were observed for SNAP25, or NRGN (all p > 0.05) (Fig. 3 and Table 2).

Table 2
Blood biomarker changes during follow up

Biomarker	Group	Baseline (mean, SD)	Follow-up (mean, SD)	LSMean Difference (BL–FU)	95% CI	p-value	Group difference in change
GFAP	ε4/ε4	13.12 (0.55)	13.53 (0.41)	-0.387	[-0.624, -0.151]	**0.0002**	0.96
(NPQ)	ε4/ε3	12.72 (0.55)	13.20 (0.55)	-0.385	[-0.583, -0.187]	**< 0.0001**	
	ε3/ε3	12.60 (0.52)	12.99 (0.54)	-0.363	[-0.550, -0.177]	**< 0.0001**	
NfL	ε4/ε4	11.39 (0.63)	11.65 (0.51)	-0.305	[-0.578, -0.032]	**0.0204**	0.72
(NPQ)	ε4/ε3	11.18 (0.56)	11.39 (0.64)	-0.208	[-0.437, 0.021]	0.0945	
	ε3/ε3	11.14 (0.44)	11.41 (0.36)	-0.238	[-0.454, -0.022]	**0.0235**	
p-tau217	ε4/ε4	11.95 (0.33)	11.98 (0.23)	-0.096	[-0.319, 0.126]	0.7889	0.24
(NPQ)	ε4/ε3	11.75 (0.45)	11.80 (0.47)	-0.028	[-0.215, 0.158]	0.9974	
	ε3/ε3	11.53 (0.35)	11.67 (0.34)	-0.176	[-0.352, 0.0003]	0.0505	
SNAP25	ε4/ε4	12.95 (0.13)	13.00 (0.12)	-0.043	[-0.142, 0.056]	0.7934	0.84
(NPQ)	ε4/ε3	12.89 (0.11)	12.96 (0.13)	-0.069	[-0.154, 0.016]	0.1716	
	ε3/ε3	12.85 (0.10)	12.91 (0.08)	-0.055	[-0.136, 0.025]	0.3378	
NRGN	ε4/ε4	18.97 (1.34)	19.96 (0.55)	-0.957	[-2.540, 0.626]	0.4822	0.87
(NPQ)	ε4/ε3	18.64 (2.32)	19.91 (0.69)	-1.328	[-2.706, 0.051]	0.0655	
	ε3/ε3	18.47 (1.87)	19.60 (0.67)	-1.168	[-2.484, 0.148]	0.1092	

Data are presented as mean (SD) for raw values or LSMean (95% CI) for the estimated change. Sample sizes (n) refer to unique participants: Baseline, n = 60 (ε4/ε4, n = 19; ε4/ε3, n = 21; ε3/ε3, n = 20); follow-up, n = 45 (ε4/ε4, n = 11; ε4/ε3, n = 16; ε3/ε3, n = 18). Abbreviations: GFAP: glial fibrillary acidic protein; NfL: neurofilament light chain; p-tau217: phosphorylated tau 217; SNAP25: synaptosomal-associated

protein 25; NRGN: neurogranin; BL: Baseline; FU: Follow-up; LSMean: Least Squares Mean; CI: Confidence Interval; NPQ: NULISA Protein Quantification Bold values indicate p < 0.05.

Blood biomarker group differences at baseline and follow-up

At baseline, participants in ε4/ε4 exhibited significantly higher concentrations in a few biomarkers compared to ε3/ε3 (Fig. 2 and Table 3). These included GFAP: (p = 0.011, Estimate = 0.53, 95% CI [0.090–0.99]) and p-tau217: (p = 0.012, Estimate = 0.41, 95% CI [0.065–0.77]) (Table 3). No significant differences were observed at baseline between ε4/ε4 and ε4/ε3, or between ε4/ε3 and ε3/ε3, for any of the biomarkers analyzed (all p > 0.10).

Table 3
Differences in blood biomarker concentrations between groups at baseline and follow-up

Baseline	**ε4/ε4 vs. ε4/ε3**	**ε4/ε4 vs. ε3/ε3**	**ε4/ε3 vs. ε3/ε3**
	(p, Estimate, 95% CI)	**(p, Estimate, 95% CI,)**	**(p, Estimate, 95% CI)**
GFAP (NPQ)	0.10, —, —	**0.011, 0.53, [0.090–0.99]**	0.95, —, —
NfL (NPQ)	0.90, —, —	0.78, —, —	1.0, —, —
p-tau217 (NPQ)	0.69, —, —	**0.012, 0.41, [0.065–0.77]**	0.32, —, —
SNAP25 (NPQ)	0.67, —, —	0.15, —, —	0.92, —, —
NRGN (NPQ)	0.98, —, —	0.91, —, —	1.0, —, —
Follow-up	ε4/ε4 vs. ε4/ε3	ε4/ε4 vs. ε3/ε3	ε4/ε3 vs. ε3/ε3
	(p, Estimate, 95% CI)	(p, Estimate, 95% CI)	(p, Estimate, 95% CI)
GFAP (NPQ)	0.14, —, —	**0.013, 0.56, [0.085–1.04]**	0.92, —, —
NfL (NPQ)	0.63, —, —	0.58, —, —	1.0, —, —
p-tau217 (NPQ)	0.45, —, —	0.11, —, —	0.97, —, —
SNAP25 (NPQ)	0.99, —, —	0.47, —, —	0.80, —, —
NRGN (NPQ)	1.0, —, —	1.0, —, —	0.99, —, —

Results presented as p-value, estimate, [95% CI]. —: non-significant (p > 0.05). Sample sizes (n) refer to unique participants: Baseline, n = 60 (ε4/ε4, n = 19; ε4/ε3, n = 21; ε3/ε3, n = 20); follow-up, n = 45 (ε4/ε4, n = 11; ε4/ε3, n = 16; ε3/ε3, n = 18). Abbreviations: GFAP: glial fibrillary acidic protein; NfL: neurofilament light chain; p-tau217: phosphorylated tau 217; SNAP25: synaptosomal-associated protein 25; NRGN: neurogranin; CI: Confidence Interval; NPQ: NULISA Protein Quantification Bold values indicate p < 0.05.

At the follow-up visit, GFAP remained the only biomarker showing a statistically significant difference between ε4/ε4 and ε3/ε3, with ε4/ε4 continuing to show higher levels (p = 0.013, Estimate = 0.56, 95%

CI [0.085–1.04]) (Fig. 2 and Table 3). The baseline differences observed for p-tau217 (p = 0.11) between ε4/ε4 and ε3/ε3 were no longer statistically significant at the follow-up time point. Similar to the baseline findings, no significant differences were found between ε4/ε4 vs. ε4/ε3 or ε4/ε3 vs. ε3/ε3 at follow-up for any marker.

Associations between baseline brain amyloid pathology and baseline blood biomarkers

Plasma p-tau217 was the only BBM significantly positively associated with brain amyloid burden, with [^{11}C]PiB SUVR explaining the highest proportion of variance (Std Beta = 0.51, p = 0.0001) (Table 4). The GFAP and NfL models were also statistically significant overall, but this was driven by demographic covariates rather than PET measures. For GFAP, age (Std Beta = 0.32, p = 0.0083) and female sex (Std Beta = − 0.37, p = 0.0023) were the significant predictors, GFAP levels being higher with higher age and in females vs. males, and for NfL, age (Std Beta = 0.31, p = 0.045) and BMI (Std Beta = − 0.36, p = 0.0069) (Table 4) were significant predictors, NfL being higher with higher age and lower BMI. No significant associations were observed for SNAP25 or NRGN (all p > 0.07) (Table 4).

Table 4

Linear Regression of Baseline Plasma Biomarkers, [^{11}C]PiB, and Clinical Predictors

Predictor	BL GFAP	BL NfL	BL p-tau217	BL SNAP25	BL NRGN
Model p	0.0001	0.0091	0.0001	0.070	0.78
Adj. R^2	0.33	0.19	0.34	—	—
AGE (estimate, 95% CI, Std Beta, p-value)	0.039 (0.011–0.069). 0.32, p = 0.0083	0.032 (0.0007 – 0.062), 0.31, p = 0.045	—, p = 0.24	—	—
APOE ε4 count (estimate, 95% CI, Std Beta, p-value)	—, p = 0.16	—, p = 0.34	—, p = 0.21	—	—
BMI (estimate, 95% CI, Std Beta, p-value)	—, p = 0.23	-0.045 (-0.077–-0.013), -0.36, p = 0.0069	—, p = 0.45	—	—
[^{11}C]PiB SUVR (estimate, 95% CI, Std Beta, p-value)	—, p = 0.090	—, p = 0.45	**0.37, (0.18–0.56)**, **0.51, p = 0.0001**	—	—
Sex (estimate, 95% CI, Std Beta, p-value)	-0.21 (-0.35–-0.074), -0.37, p = 0.0023	—, p = 0.98	—, p = 0.33	—	—

GFAP, glial fibrillary acidic protein; NfL, neurofilament light chain; p-tau217, phosphorylated tau at threonine 217; SNAP25, synaptosomal-associated protein 25; NRGN, neurogranin; BMI, body mass index; PiB SUVR, Pittsburgh compound B standardized uptake value ratio (cortical composite region). Values are β coefficients (estimate) with 95% CI, p-values and Standardized Beta derived from multivariable linear regression models for each biomarker outcome. n = 60 unique participants (baseline visit). Bold values indicate $p < 0.05$.

Associations between baseline amyloid pathology and follow-up blood biomarkers

At the follow-up visit, plasma p-tau217 remained the only BBM significantly associated with brain amyloid burden. [^{11}C]PiB SUVR was the only significant predictor of p-tau217 (Std Beta = 0.63, p = 0.0001) (Table 5). The GFAP and NfL models were again statistically significant overall, but as at

baseline, this was driven by demographic covariates rather than PET measures. For GFAP, age (Std Beta = 0.33, p = 0.030) and sex (Std Beta = − 0.32, p = 0.032) were the significant predictors. For NfL, BMI was the only significant predictor (Std Beta = − 0.57, p < 0.0001) (Table 5). No significant associations were observed for SNAP25 or NRGN (both p > 0.18) (Table 5).

Table 5

Linear Regression of Follow-up Plasma Biomarkers, [^{11}C]PiB SUVR, and Clinical Predictors

Predictor	**FU GFAP**	**FU NfL**	**FU p-tau217**	**FU SNAP25**	**FU NRGN**
Model p	0.0091	0.0004	0.0023	0.18	0.35
Adj. R^2	0.25	0.39	0.31	—	—
AGE (estimate, 95% CI, Std Beta, p-value)	0.038, (0.0040–0.073), 0.33, p = 0.030	—, p = 0.19	—, p = 0.89	—	—
APOE ε4 count (estimate, 95% CI, Std Beta, p-value)	—, p = 0.27	—, p = 0.69	—, p = 0.75	—	—
BMI (estimate, 95% CI, Std Beta, p-value)	—, p = 0.14	-0.069, (-0.10–-0.037), -0.57, p < 0.0001	—, p = 0.55	—	—
[^{11}C]PiB SUVR (estimate, 95% CI, Std Beta, p-value)	—, p = 0.42	—, p = 0.95	**0.47, (0.25–0.69), 0.63, p = 0.0001**	—	—
Sex (estimate, 95% CI, Std Beta, p-value)	-0.20, (-0.37–-0.017), -0.32, p = 0.032	—, p = 0.17	—, p = 0.40	—	—

GFAP, glial fibrillary acidic protein; NfL, neurofilament light chain; p-tau217, phosphorylated tau at threonine 217; SNAP25, synaptosomal-associated protein 25; NRGN, neurogranin; BMI, body mass index; PiB SUVR, Pittsburgh compound B standardized uptake value ratio (cortical composite region). Values are β coefficients (estimate) with 95% CI, p-values and Standardized Beta derived from multivariable linear regression models for each biomarker outcome. n = 45 unique participants (follow-up visit). Bold values indicate p < 0.05.

Associations between synaptic density (UCB-J visit) and follow-up blood biomarkers

At follow-up, no BBM was significantly associated with synaptic density as measured by [^{11}C]UCB-J SUVR alone. The models for GFAP and NfL were statistically significant overall ($p = 0.031$ and $p < 0.0001$, respectively), but as with the amyloid PET models, the GFAP result was driven by demographic covariates rather than the PET measure. For GFAP, age (Std Beta = 0.39, $p = 0.034$) and sex (Std Beta = − 0.40, $p = 0.029$) were the significant predictors, while [^{11}C]UCB-J SUVR was not ($p = 0.97$) (Additional file 1: Table S2). For NfL, both BMI (Std Beta = − 0.62, $p < 0.0001$) and [^{11}C]UCB-J SUVR (Std Beta = 0.33, $p = 0.012$) were significant predictors, with the model explaining a substantial proportion of variance (Adj. $R^2 = 0.50$) (Additional file 1: Table S2). No significant associations with [^{11}C]UCB-J SUVR or demographic covariates were observed for p-tau217, SNAP25, or NRGN (all $p > 0.21$) (Additional file 1: Table S2).

Blood biomarker associations with neuroinflammation

None of the BBMs were significantly associated with baseline neuroinflammation as measured by [^{11}C]PK11195 DVR, either at baseline or follow-up. Where overall model significance was observed, this was driven by covariates rather than the PET measure. For GFAP, age and sex were significant predictors, and for NfL, BMI was a significant predictor, mirroring the pattern seen in the amyloid and synaptic density models. In the baseline models, which did not include [^{11}C]PiB SUVR, *APOE* ε4 count was additionally associated with GFAP (Std Beta = 0.34, $p = 0.0063$) and p-tau217 (Std Beta = 0.40, $p = 0.0035$). No significant associations with [^{11}C]PK11195 DVR were observed for any BBM (all $p > 0.20$) (full model results are provided in Additional file 1: Tables S3 and S4).

Discussion

The present study investigated the longitudinal relationship between core AD brain pathologies and a panel of high-sensitivity blood biomarkers in cognitively unimpaired older adults. Our primary finding is that baseline cerebral amyloid pathology was robustly associated with plasma p-tau217 levels at both baseline and follow-up, independent of age, sex, and *APOE* genotype. This supports a temporally ordered relationship in which amyloid accumulation precedes and is closely associated with downstream tau-related changes detectable in plasma [7]. The strong association between baseline amyloid burden and follow-up p-tau217 levels further reinforces the role of p-tau217 as a sensitive peripheral indicator of amyloid-driven tau-pathology, consistent with previous studies in preclinical populations [22–26]. Within the cohort, earlier cross-sectional analyses demonstrated elevated amyloid burden in *APOE* ε4 homozygotes [16], and the present longitudinal data extend these findings by showing that baseline amyloid burden, rather than genetic risk alone, is the primary determinant of subsequent tau-related changes in plasma. Notably, to our knowledge this is one of few studies to combine three distinct PET tracers assessing amyloid burden, neuroinflammation, and synaptic density with longitudinal plasma biomarkers in a genetically stratified cognitively unimpaired cohort, providing a multimodal characterization of early AD pathology rarely achieved in a single study.

In contrast to p-tau217, blood-based markers of astrogliosis and axonal injury appeared to be more strongly influenced by systemic factors, particularly age and BMI, than by baseline PET measures. Regression analyses confirmed previous reports that age and female sex were the strongest predictors of baseline GFAP [27, 28], while age and BMI were the primary predictors of baseline NfL [29, 30]. Plasma GFAP and NfL concentrations increased over time across all *APOE* groups, suggesting that rate of change in these markers may reflect more general or age-related processes rather than amyloid-specific mechanisms [31–33]. Although *APOE* ε4 homozygotes exhibited higher baseline concentrations of GFAP and p-tau217, consistent with their greater amyloid burden, the rates of longitudinal change were largely similar across genotypes. Notably, the attenuation of baseline group differences in p-tau217 at follow-up should be interpreted with caution, as selective attrition may have contributed: dropout was highest in the ε4/ε4 group (8 of 19 participants), and non-completers tended to have higher baseline amyloid burden and p-tau217 levels, although these differences were not statistically significant (Additional file 1: Table S1). This may have compressed the observed range of longitudinal change in the ε4/ε4 group. Prior studies have reported both higher levels and faster rates of p-tau217 change in cognitively healthy *APOE* ε4 carriers [34], and the discrepancy observed here may therefore relate to cohort composition or longitudinal sampling effects. Nevertheless, the persistent elevation of GFAP in ε4 homozygotes is consistent with its established association with amyloid pathology [8, 35].

Synaptic blood biomarkers demonstrated minimal longitudinal change and showed no significant association with baseline synaptic density measured by [^{11}C]UCB-J PET. Although NRGN exhibited a modest increasing trend in ε4/ε3 carriers and ε3/ε3 controls, and SNAP25 remained largely stable, these peripheral measures did not reflect the localized hippocampal synaptic loss previously observed in *APOE* ε4 homozygotes within the same cohort [17]. This discrepancy likely reflects fundamental differences in the biological processes captured by these modalities. [^{11}C]UCB-J PET quantifies the structural density of synaptic vesicle glycoprotein 2A, providing a relatively static measure of synapse abundance [36, 37], whereas circulating biomarkers such as SNAP25 and NRGN may reflect dynamic processes including synaptic turnover, dysfunction, or activity-dependent protein release [38–40]. In the earliest preclinical stages of AD, synaptic alterations may remain spatially restricted or biologically subtle, limiting their detectability in peripheral circulation even when assessed using high-sensitivity platforms such as NULISA [41, 42]. The positive association between [^{11}C]UCB-J SUVR and follow-up NfL (Std Beta = 0.33, p = 0.012) warrants comment, as it runs counter to the straightforward expectation that greater synaptic loss would predict higher circulating markers of axonal injury. Several considerations may account for this finding. First, the cortical composite ROI used for [^{11}C]UCB-J quantification reflects global cortical SV2A density and may not capture the regionally specific synaptic changes most relevant to early neurodegeneration in this cohort. Within the ASIC-E4 cohort, synaptic loss in *APOE* ε4/ε4 homozygotes has been shown to be predominantly hippocampal [17], and participants with relatively preserved cortical SV2A density may nonetheless sustain localized hippocampal or subcortical axonal injury sufficient to elevate plasma NfL. Second, NfL reflects axonal integrity broadly rather than synaptic density specifically, and in cognitively unimpaired older adults its circulating levels are driven substantially by age-related white matter and vascular processes that are biologically independent of

SV2A expression. Third, given the modest sample size available for the UCB-J analyses, the possibility that this association reflects residual confounding or a chance finding cannot be excluded. Taken together, the positive UCB-J SUVR–NfL association most likely reflects the biological and spatial dissociation between cortical synaptic density as measured by SV2A PET and the sources of axonal injury captured by peripheral NfL, rather than a paradoxical neuroprotective effect of synapse preservation. This interpretation remains speculative and should be examined in larger cohorts with regional UCB-J quantification.

This study has several strengths. The deliberate stratification by *APOE* genotype enabled systematic comparisons across varying levels of genetic AD risk in cognitively unimpaired individuals, allowing investigation of early pathological changes prior to symptom onset. The multimodal imaging approach combining amyloid, neuroinflammation, and synaptic density PET with plasma biomarkers provided a comprehensive characterization of AD-related pathology rarely achieved within a single cohort. The use of the high-sensitivity NULISA platform further strengthens the reliability of biomarker measurements, and the 4.4-year follow-up adds meaningful temporal depth by enabling assessment of biomarker trajectories rather than cross-sectional differences alone.

Limitations

Several limitations should also be acknowledged. The relatively small sample size, particularly within individual genotype subgroups, limits statistical power and may inflate effect size estimates. Dropout was highest in the *APOE* ε4/ε4 group, potentially introducing attrition bias and underestimating longitudinal changes in the highest-risk individuals. The follow-up period, while valuable, may be insufficient to capture the full trajectory of slowly progressive preclinical changes. Additionally, although all PET scans were originally planned to be acquired at the baseline visit, [^{11}C]UCB-J imaging was delayed due to tracer production difficulties and disruptions caused by the COVID-19 pandemic, resulting in a dedicated UCB-J visit separate from baseline blood sampling. This limits direct temporal alignment between synaptic density measurements and biomarker concentrations. Finally, [^{11}C]UCB-J PET was available only for a subset of participants, introducing the potential for selection bias. In addition, all participants were recruited from a single regional Finnish population, which limits the generalizability of our findings to more diverse populations in which genetic background, comorbidities and socioeconomic factors, and thereby biomarker levels and *APOE* ε4-related risk, may differ.

Conclusions

In summary, these findings support a temporally and mechanistically stratified model of preclinical AD, in which plasma p-tau217 tracks amyloid-driven pathological progression early and specifically, while markers of astrogliosis and axonal injury reflect broader age-related processes with a less direct relationship to amyloid burden. The relative insensitivity of circulating synaptic biomarkers at this stage likely reflects the spatial restriction and biological subtlety of early synaptic alterations rather than a failure of the platform. These results reinforce the utility of plasma p-tau217 as the blood-based marker

most closely aligned with the amyloid-tau axis in cognitively unimpaired individuals, while also underscoring that a single biomarker cannot capture the full complexity of preclinical AD. Future longitudinal studies with longer follow-up and reduced attrition will be needed to determine whether divergent biomarker trajectories across *APOE* genotypes emerge over time and at what stage synaptic markers become informative in peripheral circulation.

Abbreviations

AD, Alzheimer's disease; APOE, apolipoprotein E; BBM, blood-based biomarker; BL, baseline; BMI, body mass index; CI, confidence interval; DVR, distribution volume ratio; EDTA, ethylenediaminetetraacetic acid; FU, follow-up; GFAP, glial fibrillary acidic protein; HSD, honest significant difference; IQR, interquartile range; LLM, large language model; LSMean, least squares mean; MMSE, Mini-Mental State Examination; MRI, magnetic resonance imaging; NfL, neurofilament light chain; NPQ, NULISA Protein Quantification; NRGN, neurogranin; NULISA, nucleic acid-linked immuno-sandwich assay; p-tau217, tau phosphorylated at threonine 217; PET, positron emission tomography; PiB, Pittsburgh compound B; Q-Q, quantile-quantile; ROI, region of interest; SD, standard deviation; SNAP25, synaptosomal-associated protein 25; Std Beta, standardized beta coefficient; SUVR, standardized uptake value ratio; SV2A, synaptic vesicle glycoprotein 2A; TSPO, 18-kDa translocator protein.

Declarations

Ethics approval and consent to participate

The study was conducted in accordance with the Declaration of Helsinki and was approved by the Ethical Committee of the Hospital District of Southwest Finland. All participants provided written informed consent before taking part in the study.

Consent for publication

Not applicable.

Availability of data and materials

The data used during the current study are available to qualified researchers from the corresponding author on reasonable request.

Competing interests

HZ has served at scientific advisory boards and/or as a consultant for Abbvie, Acumen, Alamar, Alector, Alzinova, ALZpath, Amylyx, Annexon, Apellis, Artery Therapeutics, AZTherapies, Bioventix, Cognitact, Cognito Therapeutics, CogRx, Denali, Eisai, Enigma, Johnson & Johnson, LabCorp, Merck Sharp & Dohme, Merry Life, Nervgen, New Amsterdam, Novo Nordisk, Optoceutics, Passage Bio, Pinteon Therapeutics, Prothena, Quanterix, Red Abbey Labs, reMYND, Roche, Samumed, ScandiBio Therapeutics

AB, Siemens Healthineers, Triplet Therapeutics, and Wave, has given lectures sponsored by Alzecure, BioArctic, Biogen, Cellectricon, Fujirebio, LabCorp, Lilly, Novo Nordisk, Oy Medix Biochemica AB, Roche, and WebMD, is a co-founder of Brain Biomarker Solutions in Gothenburg AB (BBS), which is a part of the GU Ventures Incubator Program, and is a shareholder of CERimmune Therapeutics (outside submitted work). MK, AS, LE, AB and JOR declare that they have no competing interests.

Funding

The ASIC-E4 study was supported by Finnish Governmental Research Funding for Turku University Hospital. AS received personal grants related to this study from the Research Council of Finland [grant number 341059], the Emil Aaltonen Foundation, the Paulo Foundation, and the Orion Research Foundation sr. LE was supported by the Finnish Medical Foundation, the Emil Aaltonen Foundation, the Paulo Foundation, the Juho Vainio Foundation, and Finnish Governmental Research Funding. JOR received funding from the Research Council of Finland [grant number 310962], the Sigrid Jusélius Foundation, and Finnish Governmental Research Funding for Turku University Hospital. MK was supported by the Yrjö Jahnsson Foundation. HZ is a Wallenberg Scholar and a Distinguished Professor at the Swedish Research Council supported by grants from the Swedish Research Council [grant numbers 2023-00356, 2022-01018 and 2019-02397], the European Union's Horizon Europe research and innovation programme [grant agreement number 101053962], Swedish State Support for Clinical Research [grant number ALFGBG-71320], the Alzheimer Drug Discovery Foundation, USA [grant number 201809-2016862], the Alzheimer's Disease Strategic Fund and the Alzheimer's Association [grant numbers ADSF-21-831376-C, ADSF-21-831381-C, ADSF-21-831377-C and ADSF-24-1284328-C], the European Partnership on Metrology, co-financed from the European Union's Horizon Europe Research and Innovation Programme and by the Participating States [NEuroBioStand, grant number 22HLT07], the Bluefield Project, Cure Alzheimer's Fund, the Olav Thon Foundation, the Erling-Persson Family Foundation, Familjen Rönströms Stiftelse, Familjen Beiglers Stiftelse, Stiftelsen för Gamla Tjänarinnor, Hjärnfonden, Sweden [grant number FO2022-0270], the European Union's Horizon 2020 research and innovation programme under the Marie Skłodowska-Curie grant agreement [grant number 860197, MIRIADE], the European Union Joint Programme for Neurodegenerative Disease Research [grant number JPND2021-00694], the National Institute for Health and Care Research University College London Hospitals Biomedical Research Centre, the UK Dementia Research Institute at University College London [grant number UKDRI-1003], and an anonymous donor. The funders had no role in the study design; in the collection, analysis and interpretation of data; in the writing of the report; or in the decision to submit the article for publication.

Authors' contributions

M.K., J.O.R and A.S. designed the study concept. M.K. drafted the manuscript. M.K., A.S., and L.L.E., contributed to data collection. M.K. and A.B. analyzed data. M.K., J.O.R, A.S., L.L.E, and H.Z., contributed to study design and interpretation of the data. J.O.R., A.S., and H.Z. supervised the study. All authors read and critically revised the manuscript for its content and approved the final submitted version.

Acknowledgements

The participants of the study are warmly acknowledged for their commitment to the study. The authors would also like to acknowledge the staff of Turku PET Centre data collection for this study.

References

1. Villemagne VL, Burnham S, Bourgeat P, Brown B, Ellis KA, Salvado O, et al. Amyloid β deposition, neurodegeneration, and cognitive decline in sporadic Alzheimer's disease: a prospective cohort study. Lancet Neurol. 2013;12:357–67. 10.1016/S1474-4422(13)70044-9.
2. Selkoe DJ, Hardy J. The amyloid hypothesis of Alzheimer's disease at 25 years. EMBO Mol Med. 2016;8:595–608. 10.15252/emmm.201606210.
3. Crous-Bou M, Minguillón C, Gramunt N, Molinuevo JL. Alzheimer's disease prevention: from risk factors to early intervention. Alzheimers Res Ther. 2017;9:71. 10.1186/s13195-017-0297-z.
4. Corder EH, Saunders AM, Strittmatter WJ, Schmechel DE, Gaskell PC, Small GW, et al. Gene dose of apolipoprotein E type 4 allele and the risk of Alzheimer's disease in late onset families. Science. 1993;261:921–3. 10.1126/science.8346443.
5. Saunders AM, Strittmatter WJ, Schmechel D, St George-Hyslop PH, Pericak-Vance MA, Joo SH, et al. Association of apolipoprotein E allele epsilon 4 with late-onset familial and sporadic Alzheimer's disease. Neurology. 1993;43:1467–72. 10.1212/wnl.43.8.1467.
6. Zetterberg H, Bendlin BB. Biofluid biomarkers in Alzheimer's disease and other neurodegenerative dementias. Nature. 2026;650:49–59. 10.1038/s41586-025-10018-w.
7. De Strooper B, Zetterberg H. Tracking the turning point in Alzheimer's disease. Science. 2026;392:468–9. 10.1126/science.aeb6987.
8. Benedet AL, Milà-Alomà M, Vrillon A, Ashton NJ, Pascoal TA, Lussier F, et al. Differences between plasma and cerebrospinal fluid glial fibrillary acidic protein levels across the Alzheimer disease continuum. JAMA Neurol. 2021;78:1471–83. 10.1001/jamaneurol.2021.3671.
9. Parvizi T, König T, Wurm R, Silvaieh S, Altmann P, Klotz S, et al. Real-world applicability of glial fibrillary acidic protein and neurofilament light chain in Alzheimer's disease. Front Aging Neurosci. 2022;14:887498. 10.3389/fnagi.2022.887498.
10. Wang X, Shi Z, Qiu Y, Sun D, Zhou H. Peripheral GFAP and NfL as early biomarkers for dementia: longitudinal insights from the UK Biobank. BMC Med. 2024;22:192. 10.1186/s12916-024-03418-8.
11. Cheng Q, Fan Y, Zhang P, Liu H, Han J, Yu Q, et al. Biomarkers of synaptic degeneration in Alzheimer's disease. Ageing Res Rev. 2025;104:102642. 10.1016/j.arr.2024.102642.
12. Colom-Cadena M, Spires-Jones T, Zetterberg H, Blennow K, Caggiano A, DeKosky ST, et al. The clinical promise of biomarkers of synapse damage or loss in Alzheimer's disease. Alzheimers Res Ther. 2020;12:21. 10.1186/s13195-020-00588-4.
13. Planalp EM, Langhough RE, Jonaitis EM, Van Hulle CA, Wilson RE, Kollmorgen G, et al. Synaptic markers are associated with cognitive decline after accounting for amyloid burden among an at-risk

Alzheimer's disease cohort. Sci Rep. 2025;15:19399. 10.1038/s41598-025-04319-3.

14. Roveta F, Cermelli A, Boschi S, Ferrandes F, Grassini A, Marcinnò A, et al. Synaptic proteins as fluid biomarkers in Alzheimer's disease: a systematic review and meta-analysis. J Alzheimers Dis. 2022;90:1381–93. 10.3233/JAD-220515.
15. Snellman A, Ekblad LL, Koivumäki M, Lindgrén N, Tuisku J, Perälä M, et al. ASIC-E4: interplay of beta-amyloid, synaptic density and neuroinflammation in cognitively normal volunteers with three levels of genetic risk for late-onset Alzheimer's disease – study protocol and baseline characteristics. Front Neurol. 2022;13:826423. 10.3389/fneur.2022.826423.
16. Snellman A, Ekblad LL, Tuisku J, Koivumäki M, Ashton NJ, Lantero-Rodriguez J, et al. APOE ε4 gene dose effect on imaging and blood biomarkers of neuroinflammation and beta-amyloid in cognitively unimpaired elderly. Alzheimers Res Ther. 2023;15:71. 10.1186/s13195-023-01209-6.
17. Snellman A, Tuisku J, Koivumäki M, Wahlroos S, Aarnio R, Rajander J, et al. SV2A PET shows hippocampal synaptic loss in cognitively unimpaired APOE ε4/ε4 homozygotes. Alzheimers Dement. 2024;20:8802–13. 10.1002/alz.14327.
18. Koivumäki M, Ekblad L, Lantero-Rodriguez J, Ashton NJ, Karikari TK, Helin S, et al. Blood biomarkers of neurodegeneration associate differently with amyloid deposition, medial temporal atrophy, and cerebrovascular changes in APOE ε4-enriched cognitively unimpaired elderly. Alzheimers Res Ther. 2024;16:112. 10.1186/s13195-024-01477-w.
19. Karjalainen T, Tuisku J, Santavirta S, Kantonen T, Bucci M, Tuominen L, et al. Magia: robust automated image processing and kinetic modeling toolbox for PET neuroinformatics. Front Neuroinform. 2020;14:3. 10.3389/fninf.2020.00003.
20. Turkheimer FE, Edison P, Pavese N, Roncaroli F, Anderson AN, Hammers A, et al. Reference and target region modeling of [11C]-(R)-PK11195 brain studies. J Nucl Med. 2007;48:158–67.
21. Yaqub M, Van Berckel BN, Schuitemaker A, Hinz R, Turkheimer FE, Tomasi G, et al. Optimization of supervised cluster analysis for extracting reference tissue input curves in (R)-[11C]PK11195 brain PET studies. J Cereb Blood Flow Metab. 2012;32:1600–8. 10.1038/jcbfm.2012.59.
22. Mattsson-Carlgren N, Janelidze S, Bateman RJ, Smith R, Stomrud E, Serrano GE, et al. Soluble P-tau217 reflects amyloid and tau pathology and mediates the association of amyloid with tau. EMBO Mol Med. 2021;13:e14022. 10.15252/emmm.202114022.
23. Milà-Alomà M, Ashton NJ, Shekari M, Salvadó G, Ortiz-Romero P, Montoliu-Gaya L, et al. Plasma p-tau231 and p-tau217 as state markers of amyloid-β pathology in preclinical Alzheimer's disease. Nat Med. 2022;28:1797–801. 10.1038/s41591-022-01925-w.
24. Salvadó G, Janelidze S, Bali D, Dolado AO, Therriault J, Brum WS, et al. Plasma phosphorylated tau 217 to identify preclinical Alzheimer disease. JAMA Neurol. 2025;82:1122–34. 10.1001/jamaneurol.2025.3217.
25. Malek-Ahmadi M, Sharma S, Stipho F, Denkinger M, Singh A, Brum WS, et al. Plasma phosphorylated tau 217 and amyloid burden in older adults without cognitive impairment: a meta-analysis. JAMA Neurol. 2026;83:13–9. 10.1001/jamaneurol.2025.4721.

26. Palmqvist S, Janelidze S, Quiroz YT, Zetterberg H, Lopera F, Stomrud E, et al. Discriminative accuracy of plasma phospho-tau217 for Alzheimer disease vs other neurodegenerative disorders. JAMA. 2020;324:772–81. 10.1001/jama.2020.12134.
27. Gonzales MM, Vela G, Philip V, Trevino H, LaRoche A, Wang CP, et al. Demographic and clinical characteristics associated with serum GFAP levels in an ethnically diverse cohort. Neurology. 2023;101:e1531–41. 10.1212/WNL.0000000000207706.
28. Thaker AA, McConnell BV, Rogers DM, Carlson NE, Coughlan C, Jensen AM, et al. Astrogliosis, neuritic microstructure, and sex effects: GFAP is an indicator of neuritic orientation in women. Brain Behav Immun. 2023;113:124–35. 10.1016/j.bbi.2023.06.026.
29. Koini M, Pirpamer L, Hofer E, Buchmann A, Pinter D, Ropele S, et al. Factors influencing serum neurofilament light chain levels in normal aging. Aging. 2021;13:25729–38. 10.18632/aging.203790.
30. Manouchehrinia A, Piehl F, Hillert J, Kuhle J, Alfredsson L, Olsson T, et al. Confounding effect of blood volume and body mass index on blood neurofilament light chain levels. Ann Clin Transl Neurol. 2020;7:139–43. 10.1002/acn3.50972.
31. Khalil M, Pirpamer L, Hofer E, Voortman MM, Barro C, Leppert D, et al. Serum neurofilament light levels in normal aging and their association with morphologic brain changes. Nat Commun. 2020;11:812. 10.1038/s41467-020-14612-6.
32. Rodero-Romero A, Monreal E, Sainz-Amo R, García Domínguez JM, Villarrubia N, Veiga-González JL, et al. Establishing normal serum values of neurofilament light chains and glial fibrillary acidic protein considering the effects of age and other demographic factors in healthy adults. Int J Mol Sci. 2024;25:7808. 10.3390/ijms25147808.
33. Simrén J, Andreasson U, Gobom J, Suárez-Calvet M, Borroni B, Gillberg C, et al. Establishment of reference values for plasma neurofilament light based on healthy individuals aged 5–90 years. Brain Commun. 2022;4:fcac174. 10.1093/braincomms/fcac174.
34. Martínez-Dubarbie F, Guerra-Ruiz A, López-García S, Lage C, Fernández-Matarrubia M, Pozueta-Cantudo A, et al. Longitudinal trajectory of plasma p-tau217 in cognitively unimpaired subjects. Alzheimers Res Ther. 2024;16:268. 10.1186/s13195-024-01642-1.
35. Snellman A, Ekblad L, Ashton N, Karikari T, Lantero-Rodriguez J, Pietilä E, et al. Head-to-head comparison of plasma p-tau181, p-tau231 and glial fibrillary acidic protein in clinically unimpaired elderly with three levels of APOE4-related risk for Alzheimer's disease. Neurobiol Dis. 2023;183:106175. 10.1016/j.nbd.2023.106175.
36. Finnema SJ, Nabulsi NB, Eid T, Detyniecki K, Lin SF, Chen MK, et al. Imaging synaptic density in the living human brain. Sci Transl Med. 2016;8:348ra96. 10.1126/scitranslmed.aaf6667.
37. Mecca AP, Chen MK, O'Dell RS, Naganawa M, Toyonaga T, Godek TA, et al. In vivo measurement of widespread synaptic loss in Alzheimer's disease with SV2A PET. Alzheimers Dement. 2020;16:974–82. 10.1002/alz.12097.

38. Brinkmalm A, Brinkmalm G, Honer WG, Frölich L, Hausner L, Minthon L, et al. SNAP-25 is a promising novel cerebrospinal fluid biomarker for synapse degeneration in Alzheimer's disease. Mol Neurodegener. 2014;9:53. 10.1186/1750-1326-9-53.
39. Kvartsberg H, Lashley T, Murray CE, Brinkmalm G, Cullen NC, Höglund K, et al. The intact postsynaptic protein neurogranin is reduced in brain tissue from patients with familial and sporadic Alzheimer's disease. Acta Neuropathol. 2019;137:89–102. 10.1007/s00401-018-1910-3.
40. Zetterberg H, Schott JM. Blood biomarkers for Alzheimer's disease and related disorders. Acta Neurol Scand. 2022;146:51–5. 10.1111/ane.13628.
41. Lista S, Santos-Lozano A, Emanuele E, Mercuri NB, Gabelle A, López-Ortiz S, et al. Monitoring synaptic pathology in Alzheimer's disease through fluid and PET imaging biomarkers: a comprehensive review and future perspectives. Mol Psychiatry. 2024;29:847–57. 10.1038/s41380-023-02376-6.
42. Ribarič S. Detecting early cognitive decline in Alzheimer's disease with brain synaptic structural and functional evaluation. Biomedicines. 2023;11:355. 10.3390/biomedicines11020355.

Figures

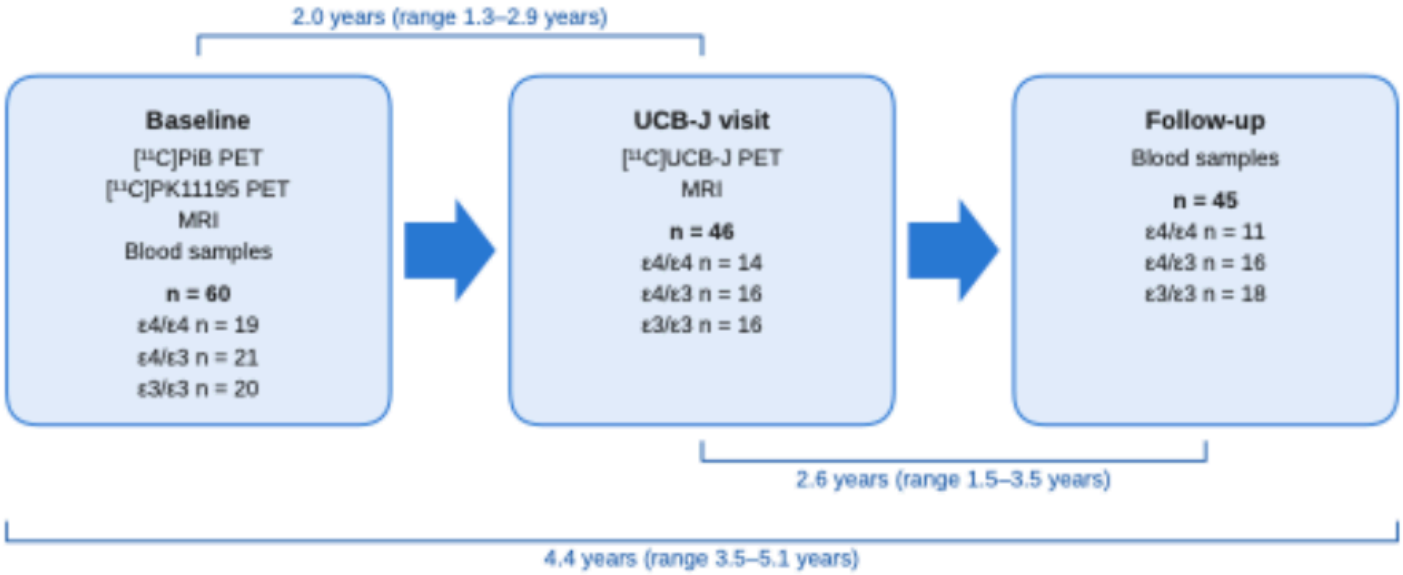


Figure 1

Study design and participant flow. Timeline of the baseline visit ([11C]PiB PET, [11C]PK11195 PET, MRI and blood sampling), the separate UCB-J visit ([11C]UCB-J PET and MRI) and the follow-up visit (blood sampling), with the number of participants in each APOE genotype group. Intervals are given as mean (range). Sample sizes (n) refer to unique participants: baseline, n = 60 (ε4/ε4, n = 19; ε4/ε3, n = 21; ε3/ε3, n = 20); UCB-J visit, n = 46 (ε4/ε4, n = 14; ε4/ε3, n = 16; ε3/ε3, n = 16); follow-up, n = 45 (ε4/ε4, n = 11; ε4/ε3, n = 16; ε3/ε3, n = 18). MRI, magnetic resonance imaging; PET, positron emission tomography.

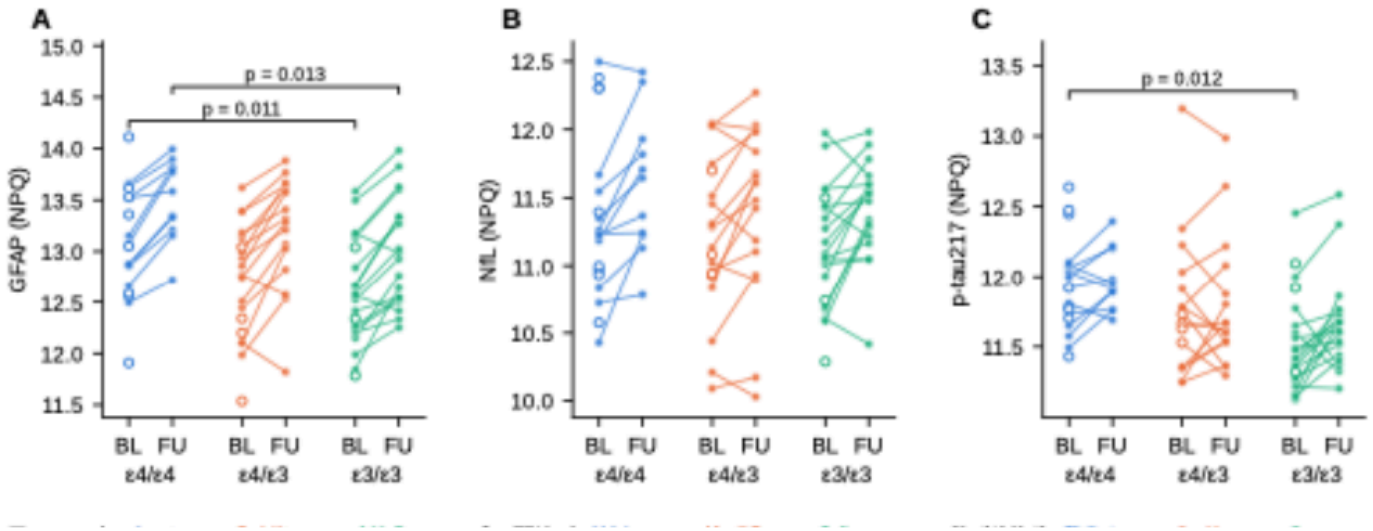


Figure 2

Individual longitudinal changes in plasma GFAP (A), NfL (B) and p-tau217 (C) by APOE genotype. Each line connects one participant's baseline and follow-up values. Brackets show significant pairwise differences between ε4/ε4 and ε3/ε3 at baseline and follow-up (Table 3). BL, baseline; FU, follow-up. Sample sizes (n) refer to unique participants: baseline, n = 60 (ε4/ε4, n = 19; ε4/ε3, n = 21; ε3/ε3, n = 20); follow-up, n = 45 (ε4/ε4, n = 11; ε4/ε3, n = 16; ε3/ε3, n = 18). GFAP, glial fibrillary acidic protein; NfL, neurofilament light chain; NPQ, NULISA Protein Quantification (log2 scale); p-tau217, tau phosphorylated at threonine 217.

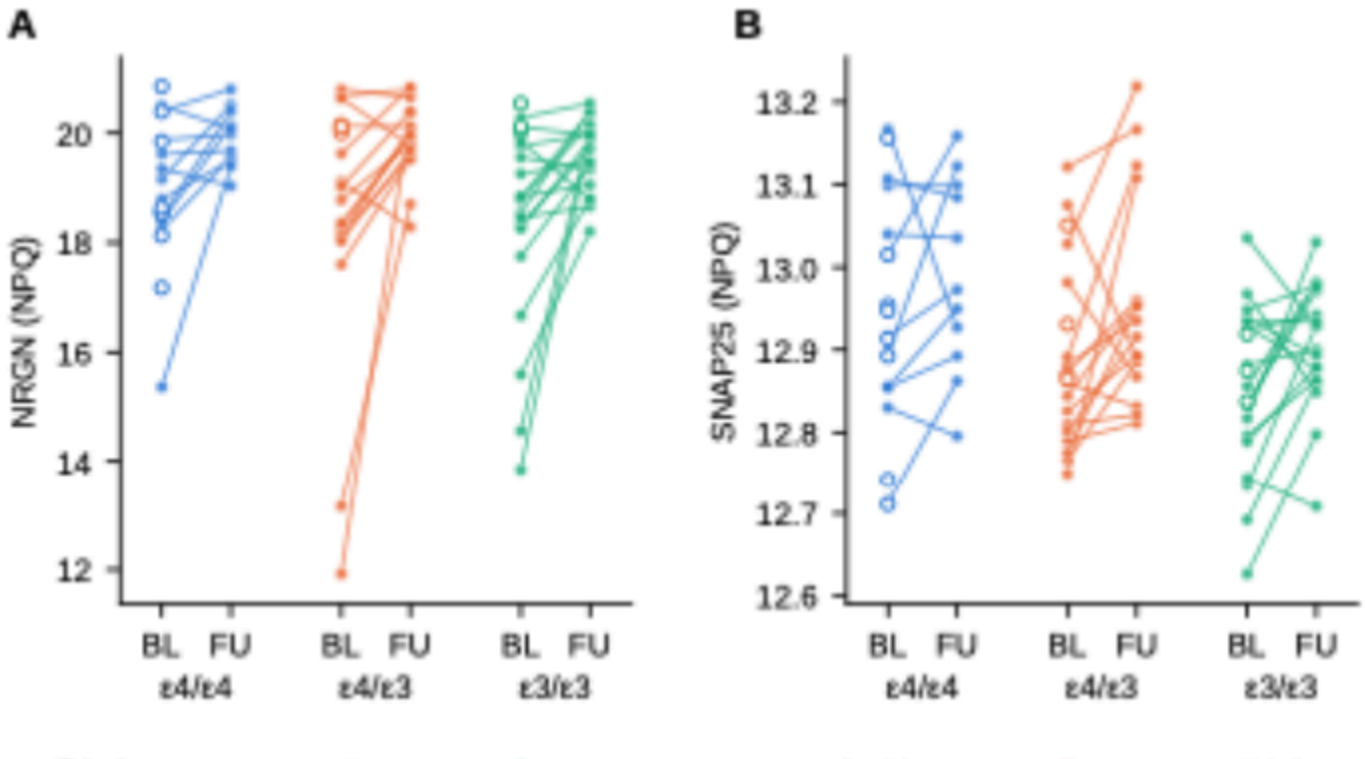


Figure 3

Individual longitudinal changes in plasma NRGN (A) and SNAP25 (B) by APOE genotype. Each line connects one participant's baseline and follow-up values. BL, baseline; FU, follow-up. Sample sizes (n) refer to unique participants: baseline, n = 60 (ε4/ε4, n = 19; ε4/ε3, n = 21; ε3/ε3, n = 20); follow-up, n = 45 (ε4/ε4, n = 11; ε4/ε3, n = 16; ε3/ε3, n = 18). NPQ, NULISA Protein Quantification (log2 scale); NRGN, neurogranin; SNAP25, synaptosomal-associated protein 25.

Supplementary Files

This is a list of supplementary files associated with this preprint. Click to download.

- Additionalfile1.docx